TITLE: Pre-clinical search of SARS-CoV-2 inhibitors and their combinations in approved drugs to tackle COVID-19 pandemic

AUTHORS: Jordi Rodon[1], Jordana Muñoz-Basagoiti[2,*], Daniel Perez-Zsolt[2,*], Marc Noguera-Julian[2,7], Roger Paredes[2,6], Lourdes Mateu[6], Carles Quiñones[6], Itziar Erkizia[2], Ignacio Blanco[5], Alfonso Valencia[3,4], Víctor Guallar[3,4], Jorge Carrillo[2], Julià Blanco[2,5,7], Joaquim Segalés[8,9], Bonaventura Clotet[2,5,7], Júlia Vergara-Alert[1,+], Nuria Izquierdo-Useros[2,5,+]

*Equal contribution

[+] Dual senior authorship

Corresponding authors: JV-A: julia.vergara@irta.cat and NI-U nizquierdo@irsicaixa.es

Affiliations: [1]IRTA, Centre de Recerca en Sanitat Animal (CReSA, IRTA-UAB), Campus de la UAB, 08193 Bellaterra (Cerdanyola del Vallès), Spain

[2]IrsiCaixa AIDS Research Institute, 08916, Badalona, Spain

[3]Barcelona Supercomputing Center

[4]Catalan Institution for Research and Advanced Studies (ICREA), Barcelona, Spain

[5]Germans Trias i Pujol Research Institute (IGTP), Can Ruti Campus, 08916, Badalona, Spain

[6]Germans Trias i Pujol Hospital, Badalona, Catalonia, Spain

[7]University of Vic–Central University of Catalonia (UVic-UCC), Vic, Spain

[8]UAB, CReSA (IRTA-UAB), Campus de la UAB, 08193 Bellaterra (Cerdanyola del Vallès), Spain

[9]Departament de Sanitat i Anatomia Animals, Facultat de Veterinària, UAB, 08193 Bellaterra (Cerdanyola del Vallès), Spain

ABSTRACT (237)

There is an urgent need to identify novel drugs against the new coronavirus. Although different antivirals are given for the clinical management of SARS-CoV-2 infection, their efficacy is still under evaluation. Here, we have screened existing drugs approved for human use in a variety of diseases, to compare how they counteract SARS-CoV-2-induced cytopathic effect and viral replication *in vitro.* Among the potential 72 antivirals tested herein that were previously proposed to inhibit SARS-CoV-2 infection, only 18% had *in vitro* antiviral activity. Moreover, only eight families had an IC_{50} below 25 µM or 10^2 IU/mL. These include chloroquine derivatives and remdesivir, along with plitidepsin, cathepsin inhibitors, nelfinavir mesylate hydrate, interferon 2-alpha, interferon-gamma, fenofibrate and camostat. Plitidepsin was the only clinically approved drug displaying nanomolar efficacy. Four of these families, including novel cathepsin inhibitors, blocked viral entry in a cell-type specific manner. Since the most effective antivirals usually combine therapies that tackle the virus at different steps of infection, we also assessed several drug combinations. Although no particular synergy was found, inhibitory combinations did not reduce their antiviral activity. Thus, these combinations could decrease the potential emergence of resistant viruses. Antivirals prioritized herein identify novel compounds and their mode of action, while independently replicating the activity of a reduced proportion of drugs which are mostly approved for clinical use. Combinations of these drugs should be tested in animal models to inform the design of fast track clinical trials.

INTRODUCTION

A novel betacoronavirus, the severe acute respiratory syndrome coronavirus 2 (SARS-CoV-2), is causing a respiratory disease pandemic that began in Wuhan, China, in November 2019, and has now spread across the world (Chen et al., 2020). To date, remdesivir is the only approved antiviral drug for the specific treatment of this coronavirus infectious disease 2019 or COVID-19 (Beigel et al., 2020; Grein et al., 2020). However, several drugs are being used in the frontline of clinical management of SARS-CoV-2-infected individuals in hospitals all around the world, to try to avoid the development of the COVID-19 associated pneumonia, which can be fatal. By the end of September 2020, almost a million people had died from COVID-19, and over 32 million people have been infected (WHO situation report).

Although different drug regimens are being applied to hospitalized patients, no clinical study has evidenced their efficacy yet. Under this scenario, initiatives launched by the World Health Organization (WHO), such as the SOLIDARITY study that has compared remdesivir, hydroxychloroquine, ritonavir/lopinavir and ritonavir/lopinavir plus ß-interferon regimes, have been of critical importance to prioritize the use of the most active compounds (WHO, 2020). Unfortunately, although remdesivir has proven efficacy in randomized controlled trials (Beigel et al., 2020; Grein et al., 2020), a recent update of the WHO clinical trial has failed to detect any effect on overall mortality, initiation of ventilation and duration of hospital stay with any of the antivirals tested (Pan et al., 2020). Thus, there is an urgent need to identify novel therapeutic approaches for individuals with COVID-19 developing severe disease and fatal outcomes.

In this report we present a prioritized list of effective compounds with proven antiviral efficacy *in vitro* to halt SARS-CoV-2 replication. Compounds were analyzed depending on their expected mechanism of action, to identify candidates tackling diverse steps of the viral life cycle. SARS-CoV-2 entry requires viral binding and spike protein activation via interaction with the cellular receptor ACE2 and the cellular protease TMPRSS2 (Hoffmann et al., 2020), a mechanism favored by viral internalization via endocytosis. Interference with either of these processes has proven to decrease SARS-CoV-2 infectivity (Hoffmann et al., 2020; Monteil et al.2020), and therefore, inhibitors targeting viral entry may prove valuable. In addition, SARS-CoV-2 enters into the cells via endocytosis and accumulates in endosomes where cellular cathepsins can also prime the

spike protein and favor viral fusion upon cleavage (Hoffmann et al., 2020; Mingo et al., 2015; Simmons et al., 2005), providing additional targets for antiviral activity. Once SARS-CoV-2 fuses with cellular membranes, it triggers viral RNA release into the cytoplasm, where polyproteins are translated and cleaved by proteases (Song et al., 2019). This leads to the formation of an RNA replicase-transcriptase complex driving the production of negative-stranded RNA via both replication and transcription (Song et al., 2019). Negative-stranded RNA transcribes into positive RNA genomes, allowing for the translation of viral nucleoproteins, which assemble in viral capsids at the cytoplasm (Song et al., 2019). These capsids then bud into the lumen of endoplasmic reticulum (ER)-Golgi compartments, where viruses are finally released into the extracellular space by exocytosis. Potentially, any of these viral cycle steps could be targeted with antivirals, so we have thus searched for these compounds as well.

Finally, as the most effective antiviral treatments are usually based on combined therapies that tackle distinct steps of the viral life cycle, we also tested the active compounds in combination. These combinations may be critical to abrogate the potential emergence of resistant viruses and to increase antiviral activity, enhancing the chances to improve clinical outcome.

RESULTS

We have tested the antiviral activity of different clinically available compounds and their combinations by assessing their ability to inhibit viral induced cytopathic effect *in vitro*. Our strategy was circumscribed mostly to compounds approved for clinical use, since they are ideal candidates for entering into fast track clinical trials. Drug selection criteria first focused on compounds already being tested in clinical trials, along with well-known human immunodeficiency virus-1 (HIV-1) and hepatitis C virus (HCV) protease inhibitors, as well as other compounds suggested to have potential activity against SARS-CoV-2 in molecular docking analysis or *in vitro* assays.

We first assessed the activity of 16 compounds with hypothetical capacity to inhibit viral entry, and then we focused on 22 drugs thought to block viral replication upon SARS-CoV-2 fusion. Molecular docking studies provided an additional 11 candidates, which were predicted to inhibit the SARS-CoV-2 main protease. Finally, 23 compounds with unknown mechanism of action were also assessed. By these means, we have compared 72 drugs and 28 of their combinations for their capacity to counteract SARS-CoV-2-induced cytopathic effect *in vitro.*

1. Antiviral activity of compounds that potentially inhibit viral entry

We first tested compounds that could have an effect before viral entry by impairing virus-cell fusion (**Supp. Table 1**). Hydroxychloroquine is an anti-malarial drug that exerts its activity by disrupting the endosome pathway, and that has been proposed as an anti-SARS-CoV-2 agent (Liu et al., 2020; Wang et al., 2020). We confirmed the inhibitory effect of hydroxychloroquine against SARS-CoV-2-induced cellular cytotoxicity on Vero E6 cells (Liu et al., 2020). A constant concentration of a clinical isolate of SARS-CoV-2 (ID EPI_ISL_510689) was mixed with increasing concentrations of hydroxychloroquine and added to Vero E6 cells. To control for drug-induced cytotoxicity, Vero E6 were also cultured with increasing concentrations of hydroxychloroquine in the absence of SARS-CoV-2. By these means we calculated the concentration at which hydroxychloroquine achieved a 50% maximal inhibitory capacity (IC_{50}). As shown in **Fig. 1A**, this drug was able to inhibit viral-induced cytopathic effects at concentrations where no cytotoxic effects of the drug were observed. The mean IC_{50} value of this drug in repeated experiments was always below 25 μM (**Supp. Table 1**). These results aligned with

previous reports highlighting the *in vitro* inhibitory capacity of chloroquine derivatives (Liu et al., 2020; Wang et al., 2020), but contrasted with data on animal models (Maisonnasse et al., 2020; Rosenke et al., 2020) or currently ongoing clinical trials that have failed to detect any associated benefit of hydroxychloroquine treatment (Boulware et al., 2020; Cavalcanti et al., 2020). Since hydroxychloroquine was first administered in combination with the antibiotic azithromycin (Gautret et al., 2020), which induces antiviral responses in bronchial epithelial cells (Gielen et al., 2010), we further tested the activity of this compound in our assay. However, in the Vero E6 model, azithromycin did not show any antiviral effect (**Fig. 1A**), and the combination of hydroxychloroquine with azithromycin had a similar activity to that of the chloroquine derivative alone (**Fig. 1A**). Indeed, this was also the case when we tested hydroxychloroquine in combination with different HIV-1 protease inhibitors and other relevant compounds currently being tested in clinical trials (**Supp. Table 2**).

Additional Food and Drug Administration (FDA)-approved compounds previously used to abrogate viral entry via clathrin-mediated endocytosis were also tested in this SARS-CoV-2-induced cytotoxicity assay (**Supp. Table 1**). Indeed, interference with clathrin-mediated endocytosis is one of the potential mechanisms by which hydroxychloroquine may exert its therapeutic effect against SARS-CoV-2 (Hu et al., 2020). One of these compounds was amantadine, which blocks coated pit invaginations at the plasma membrane (Phonphok and Rosenthal, 1991) and is licensed against influenza A virus infections and as a treatment for Parkinson's disease. In addition, we also tested chlorpromazine, an antipsychotic drug that inhibits clathrin-mediated endocytosis by preventing the assembly and disassembly of clathrin networks on cellular membranes or endosomes (Wang et al., 1993). When we assessed the antiviral efficacy of these clathrin inhibitors against SARS-CoV-2, we did not find any prominent effect; only a partial inhibition at 100 µM for amantadine (**Fig. 1B**). The broad cathepsin B/L inhibitor E64-d also showed partial inhibitory activity (**Fig. 1B**). E64-d exerts activity against viruses cleaved by cellular cathepsins upon endosomal internalization, as previously described using pseudotyped SARS-CoV-2 (Hoffmann et al., 2020). While these results could not be confirmed using the specific cathepsin B inhibitor CA-074-Me due to drug-associated toxicity (**Supp. Table 1**), it is important to highlight that none of these cathepsin inhibitors is approved for clinical use. These data suggest that SARS-CoV-2 entry in Vero E6 partially relies on clathrin-mediated endocytosis and cellular cathepsins, which cleave

the viral Spike protein and allow viral fusion once SARS-CoV-2 is internalized in endosomes. However, hydroxychloroquine antiviral activity was much more potent than that exerted by amantadine or E-64d (**Fig. 1A-B)**.

Recently, it has also been suggested that hydroxychloroquine could block SARS-CoV-2 spike interaction with GM1 gangliosides (Fantini et al., 2020). GM1 gangliosides are enriched in cholesterol domains of the plasma membrane and have been previously shown to bind to SARS-CoV spike protein (Lu et al., 2008). This mode of viral interaction is aligned with the capacity of methyl-beta cyclodextrin, which depletes cholesterol from the plasma membrane to abrogate SARS-CoV-2 induced cytopathic effect (**Fig. 1B**), as previously reported for SARS-CoV (Lu et al., 2008). Removal of cholesterol redirected ACE2 receptor to other domains, but did not alter the expression of the viral receptor (Lu et al., 2008). Moreover, NB-DNJ, an inhibitor of ganglioside biosynthesis pathway, also decreased SARS-CoV-2 cytopathic effect (**Fig. 1B**). These results highlight the possible role of gangliosides in viral binding, although the polar head group of GM3 ganglioside (3' Sialyllactose) was not able to reduce viral-induced cytopathic effect (**Supp. Table 1**).

Agents involved in autophagy, such as the BECN1-stabilizing compounds niclosamide or ciclesonide, inhibit the release of infectious SARS-CoV-2 to the supernatant (Gassen et al., 2020) or reduce the expression of viral nucleoprotein 24 h post-infection (Jeon et al., 2020). However, these autophagy inhibitors were highly toxic in our three-day assay (**Supp. Table 1**). Arbidol is a compound that intercalates into membrane lipids leading to the inhibition of membrane fusion between viruses and cells, and between viruses and endosomal membranes (Haviernik et al., 2018). Although arbidol has exhibited *in vitro* efficacy against SARS-CoV-2 (Li, 2020) it showed drug associated cytotoxicity in our assay (**Supp. Table 1**). We also tested the antiviral activity of two JAK inhibitors: baricitinib and tofacitinib. Baricitinib was previously suggested to reduce viral entry by interfering with AP2-associated protein kinase 1 (AAK1) necessary for clathrin mediated endocytosis (Richardson et al., 2020; Stebbing et al., 2020). However, neither this compound or tofacitinib protected Vero E6 cells from SARS-CoV-2 induced cytopathic effect (**Supp. Table 1**). While we did not detect an antiviral effect for JAK inhibitors, these compounds may still be useful to control hyperinflammation and cytokine storm at later stages of infection (Stebbing et al., 2020). Finally, we tested camostat, a serine protease inhibitor with capacity to abrogate SARS-CoV-2 Spike priming on the plasma

membrane of human pulmonary cells and avoid viral fusion (Hoffmann et al., 2020). Camostat showed no antiviral effect on Vero E6 cells (**Fig. 1C**), what indicates that the alternative viral endocytic route is the most prominent entry route in this renal cell type. Of note, a broader cellular protease inhibitor such as the alfa 1-antitrypsin (ATT), used to treat severe ATT human deficiency, was able to exert an antiviral effect on Vero E6. However, it required high concentrations that will most likely rely on the activity of these proteases in the endosomal route (**Fig. 1C**).

In order to confirm that previously identified compounds listed in **Supp. Table 1** specifically inhibit the viral entry step, we next employed a luciferase-based assay using pseudotyped lentivirus expressing the spike protein of SARS-CoV-2, which allows to detect viral fusion on HEK-293T cells transfected with ACE2. As a control, we used the same lentiviruses pseudotyped with a VSV glycoprotein, where no entry inhibition above 20% was detected for any of the drugs tested (data not shown). In sharp contrast, SARS-CoV-2 pseudoviruses were effectively blocked by most of the drugs previously tested on Vero E6 with wild-type virus (**Fig. 1D**). The main differences were observed with CA-074-Me, ciclesonide and arbidol. These compounds showed a partial blocking effect on ACE2 HEK-293T cells that was not obvious when using replication competent SARS-CoV-2 on Vero E6 (**Supp. Fig. 1**). In addition, NB-DNJ failed to block viral entry (**Fig. 1D**), suggesting that ganglioside dependence may be reduced in ACE2 overexpressing cells or, alternatively, that this drug requires a longer exposure time to effectively reduce the content of gangliosides via biosynthesis blocking.

Overall, using alternative SARS-CoV-2 viral systems, we could identify chloroquine derivatives, cathepsin inhibitors and cholesterol depleting agents as the most promising candidates to block SARS-CoV-2 endocytosis in Vero E6 and HEK-293T cells transfected with ACE2. However, chloroquine derivatives were the only ones that displayed an IC_{50} below 25 μM (**Supp. Table 1**), and were also active abrogating pseudoviral entry into HEK-293T cells expressing ACE2 (**Fig. 1E**). Although camostat failed to inhibit viral fusion on ACE2 HEK-293T cells (**Fig. 1E**), its activity was rescued when these cells were transfected with TMPRSS2. The opposite effect was observed for chloroquine, which reduced its inhibitory activity on TMPRSS2 transfected cells (**Fig. 1E**). Thus, the expression of cellular proteases on the plasma membrane facilitates the fusion with viral membranes, decreasing the likelihood of viral entry through the

endosomal route. These data concur with previous findings in pulmonary cells, where viral entry via endosomal route was not active since chloroquine failed to abrogate viral fusion (Maisonnasse et al., 2020); however, camostat effectively blocked this entry (Hoffmann et al., 2020). Our results highlight that alternative routes govern SARS-CoV-2 viral entry and these pathways vary depending on the cellular target. Thus, effective treatments may need to block both plasma membrane fusion and endosomal routes to fully achieve viral suppression.

2. Antiviral activity of compounds that potentially inhibit post-entry steps.

In our search for antivirals inhibiting post-viral entry steps, we first focused on remdesivir, which has *in vitro* activity against SARS-CoV-2 after viral entry (Wang et al., 2020) and has already been approved for the treatment of COVID-19 by the FDA and EMA. We further confirmed the *in vitro* capacity of remdesivir to inhibit SARS-CoV-2-induced cytopathic effect on Vero E6 (**Fig. 2A**). The mean IC_{50} value of this drug in repeated experiments was always below 10 μM (**Supp. Table 2**). In combination with hydroxychloroquine, however, remdesivir did not significantly modified its own antiviral effect (**Fig. 2B**), either when hydroxychloroquine was added at increasing concentrations or at different fixed concentrations of the drug. This was also the case for other antivirals tested in combination (**Supp. Table 2**). Of note, other RNA polymerase inhibitors such as galdesivir, which was proposed to tightly bind to SARS-CoV-2 RNA-dependent RNA polymerase (Elfiky, 2020), showed no antiviral effect (**Supp. Table 3**). Favipiravir, approved by the National Medical Products Administration of China as the first anti-COVID-19 drug in China (Tu et al., 2020), showed only partial inhibitory activity at the non-toxic concentration of 100 μM (**Supp. Table 3**).

We also assessed clinically approved protease inhibitors with potent activity against HIV-1. However, none of the HIV-1 protease inhibitors detailed in **Supp. Table 3** showed remarkable protective antiviral activity against SARS-CoV-2 infection on Vero E6 cells, with the exception of nelfinavir mesylate hydrate, which showed an IC_{50} value below 10 μM (**Supp. Table 3** and **Fig. 2C**). Lopinavir and tipranavir inhibited SARS-CoV-2-induced cytopathic effect at the non-toxic concentration of 20 μM, and amprenavir exhibited activity at the non-toxic concentration of 100 μM (**Fig. 2C**). Darunavir, which is currently being tested in ongoing clinical trials, showed partial inhibitory activity at 100 μM, although this concentration had 8.5 ± 6.2 % of cytotoxicity associated (**Fig. 2C**).

Of note, we tested HIV-1 reverse transcriptase inhibitors such as tenofovir disoproxil fumarate, emtricitabin, tenofovir alafenamide, and their combinations, but they also failed to show any antiviral effect against SARS-CoV-2 (**Supp. Fig. 1**). These results indicate that future clinical trials should contemplate the limited antiviral effect displayed by these anti-HIV-1 inhibitors against SARS-CoV-2 *in vitro*.

We also assessed the inhibitory capacity of HCV protease inhibitors, but none showed any antiviral activity (**Supp. Table 3**). Of note, exogenous interferons 2 alpha and gamma displayed antiviral activity against SARS-CoV-2 (**Supp. Table 3**). In light of these results, we tested the inhibitory effect of the TLR 7 agonist vesatolimod that triggers interferon production. Although this agonist was not able to protect from the viral-induced cytopathic effect on Vero E6 (**Supp. Table 3**), as expected since it is an interferon-producer deficient cell line (Emeny and Morgan, 1979), it could still be useful in other competent cellular targets. Since severe COVID-19 patients display impaired interferon responses (Hadjadj et al., 2020), these strategies may be valuable to avoid disease complication. In addition, we also assessed several compounds with the best computational docking scores among approved drugs against the 3CL protease of SARS-CoV-2, but none of them were effective to protect Vero E6 from viral induced cytopathic effect (**Supp. Table 4**).

The most potent antiviral tested was plitidepsin (**Fig. 2D**), which targets the eukaryotic Elongation Factor 1A2 (eEF1A2) and has been previously used for the treatment of multiple myeloma. The mean IC_{50} value of this drug in repeated experiments was always in nM concentrations (**Supp. Table 3**). In combination with other active antivirals, we did not observe a reduction on IC_{50} values (**Supp. Table 2**). This result indicates no significant synergy, but also highlights the possibility of using plitidepsin without reducing its antiviral activity in combined therapies (**Fig. 2D**), what could be relevant to avoid possible selection of resistant viruses. Overall, plitidepsin showed the lowest IC_{50} values of all the compounds tested in this *in vitro* screening (**Table 1**).

3. Antiviral activity of compounds with unknown mechanism of action.

We also assessed the inhibitory capacity of several inhibitors and broad anti-bacterial, anti-parasitic, anti-malarial, anti-influenza and anti-fungal compounds, along with other pharmacological agents previously suggested to interfere with SARS-CoV-2 infection

(**Supp. Table 5**). Such was the case of ivermectin, an FDA-approved broad spectrum anti-parasitic agent previously reported to inhibit the replication of SARS-CoV-2 *in vitro* as measured by RNA accumulation (Caly et al., 2020).

However, among these potential antivirals, only three types of molecules exerted detectable antiviral activity in our assay: itraconazole, fenofibrate, and calpain and cathepsin inhibitors such as MDL 28170 and NPO compounds. Itraconazole, an antifungal that may interfere with internal SARS-CoV-2 budding within infected cells (Wu et al., 2020), displayed an IC_{50} value of 80 μM (**Fig. 3A** and **Supp. Table 5**). Fenofibrate is clinically used to treat dyslipidemia via activation of PPARα, and also inhibited the cytopathic effect exerted by SARS-CoV-2 on Vero E6 at 20 μM (**Fig. 3B** and **Supp. Table 5**). As fenofibrate is a regulator of cellular lipid metabolism, we made use of the luciferase-based viral entry assay to try to elucidate its mode of action. When lentiviruses pseudotyped with the spike protein of SARS-CoV-2 were added to ACE-2-expressing HEK-293T cells in the presence of fenofibrate, viral entry was abrogated (**Fig. 3C**). The most potent agent found was MDL 28170, a calpain III inhibitor in a pre-clinical stage of development that displayed activity in the nanomolar range (**Fig. 3D** and **Supp. Table 5**), as previously identified *in vitro* (Riva et al., 2020). Moreover, three out of four different calpain and cathepsin inhibitors named NPO showed potent antiviral activity too (**Supp. Figure 2**). Of note, in combination with other active antivirals, we did not observe a reduction on IC_{50} values of MDL 28170 (**Supp. Table 2**).

Inhibitors of calpains, which are cysteine proteases, might impair the activity of viral proteases like 3CL (main protease) and PLpro (papain-like protease) (Riva et al., 2020; Schneider et al., 2012). However, calpain inhibitors may also inhibit cathepsin B-mediated processing of viral spike proteins or glycoproteins, including SARS-CoV and Ebola (Schneider et al., 2012; Zhou and Simmons, 2012). To understand the mechanisms of action of calpain and cathepsin inhibitors such as MDL 28170, we added lentiviruses pseudotyped with the spike protein of SARS-CoV-2 to ACE-2-expressing HEK-293T cells and the same cells also expressing TMPRSS2 in the presence of this drug. Importantly, MDL 28170 only blocked viral entry in ACE-2-expressing cells (**Fig. 3E**). This result indicates that MDL 28170 blocks cathepsins that are implicated in SARS-CoV-2 entry via the alternative endosomal pathway, as described for chloroquine

derivatives and E-64d (**Fig. 3E**), which are all active when TMPRSS2 is not present and their inhibitor camostat displays no activity (**Fig. 3E**).

In conclusion, among the 72 compounds and their 28 combinations tested herein for their potential capacity to abrogate SARS-CoV-2 cytopathic effect, we only found 22 compounds with antiviral activity, and only eight types of these drugs had an IC_{50} below 25 μM or 10^2 IU/mL (**Table 1**). These eight families of compounds were able to abrogate SARS-CoV-2 release to the supernatant in a dose dependent manner (**Fig. 4**), indicating that the reduction in the cytopathic effect that we had measured in cells correlates with viral production. As these eight families of compounds tackle different steps of the viral life cycle, they could be tested in combined therapies to abrogate the potential emergence of resistant viruses.

DISCUSSION

We have assessed the anti-SARS-CoV-2 activity of clinically approved compounds that may exert antiviral effect alone or in combination. Although we were not able to detect any remarkable synergy *in vitro*, combined therapies are key to tackle viral infections and to reduce the appearance of viral resistance. We have tested more than seventy compounds and their combinations, and verified a potent antiviral effect of hydroxychloroquine and remdesivir, along with plitidepsin, cathepsin and calpain inhibitors MDL 28179 and NPO, nelfinavir mesylate hydrate, interferon 2α, interferon-γ and fenofibrate. These are therefore the most promising agents found herein that were able to protect cells from viral-induced cytopathic effect by preventing viral replication.

Our findings highlight the utility of using hydroxychloroquine and MDL 28170 or other cathepsin inhibitors to block viral entry via the endosomal pathway in kidney cell lines such as Vero E6 or HEK-293T. However, the endosomal viral entry route is absent in pulmonary cells and, therefore, camostat should be considered as the primary inhibitor to limit SARS-CoV-2 entry in pulmonary tissues or in cells expressing TMPRSS2. These findings can explain why randomized clinical trials using hydroxychloroquine have failed to show a significant protective effect (Boulware et al., 2020; Cavalcanti et al., 2020). Nonetheless, in combined therapies, it should be noted that agents targeting the alternative endosomal SARS-CoV-2 entry route such as hydroxychloroquine or MDL 28170 could be key to stop viral dissemination in other extrapulmonary tissues where viral replication has been already detected (Hanley et al., 2020), and viral entry could take place through this endosomal pathway. This could partially explain why in a retrospective observational study including more than 2500 patients, hydroxychloroquine treatment showed a significant reduction of in-hospital mortality (Arshad et al., 2020). Thus, since alternative routes govern SARS-CoV-2 viral entry depending on the cellular target (Ou et al., 2020a), effective treatments might be needed to block both plasma membrane fusion and endosomal entry to broadly achieve viral suppression.

SARS-CoV-2 replication could be effectively blocked using nelfinavir mesylate hydrate, remdesivir and plitidepsin. While nelfinavir showed lower potency, remdesivir and plitidepsin were the most potent agents identified. However, remdesivir and plitidepsin are not yet suitable for oral delivery and require intravenous injection, complicating their clinical use for prophylaxis. Finally, we also confirmed the antiviral effect of type I and

II interferons as well as fenofibrate, which have been extensively used in the clinic for many years and may therefore prove valuable for therapeutic use.

The data presented herein should be interpreted with caution, as the IC_{50} values of drugs obtained *in vitro* may not reflect what could happen *in vivo* upon SARS-CoV-2 infection. The best antiviral compounds found in the present study need to be tested in adequate animal models. This strategy already helped to confirm the activity of remdesivir against SARS-CoV-2 (Williamson et al., 2020), while also questioning the use of hydroxychloroquine in monotherapy (Maisonnasse et al., 2020). Thus, assessing antiviral activity and safety in animal models is key to identify and advance those compounds with the highest potential to succeed in upcoming clinical trials. In turn, *in vitro* results confirmed in animal models will provide a rational basis to perform future clinical trials not only for treatment of SARS-CoV-2-infected individuals, but also for pre-exposure prophylaxis strategies that could avoid novel infections. Prophylaxis could be envisioned at a population level or to protect the most vulnerable groups, and should be implemented until an effective vaccine is developed. In particular, orally available compounds with proven safety profiles, such as fenofibrate, could represent promising agents.

MATERIAL & METHODS

Ethics statement. The institutional review board on biomedical research from Hospital Germans Trias i Pujol (HUGTiP) approved this study. The individual who provided the sample to isolate virus gave a written informed consent to participate.

Cell Cultures. Vero E6 cells (ATCC CRL-1586) were cultured in Dulbecco's modified Eagle medium, (DMEM; Lonza) supplemented with 5% fetal calf serum (FCS; EuroClone), 100 U/mL penicillin, 100 µg/mL streptomycin, and 2 mM glutamine (all ThermoFisher Scientific). HEK-293T (ATCC repository) were maintained in DMEM with 10% fetal bovine serum, 100 IU/mL penicillin and 100 µg/mL streptomycin (all from Invitrogen). HEK-293T overexpressing the human ACE2 were kindly provided by Integral Molecular Company and maintained in DMEM (Invitrogen) with 10% fetal bovine serum, 100 IU/mL penicillin and 100 µg/mL streptomycin, and 1 µg/mL of puromycin (all from Invitrogen). TMPRSS2 human plasmid (Origene) was transfected using X-tremeGENE HP Transfection Reagent (Merck) on HEK-293T overexpressing the human ACE2 and maintained in the previously described media containing 1 mg/ml of geneticin (Invitrogen) to obtain TMPRSS2/ACE2 HEK-293T cells.

Virus isolation, titration and sequencing. SARS-CoV-2 was isolated from a nasopharyngeal swab collected from an 89-year-old male patient giving informed consent and treated with Betaferon and hydroxychloroquine for 2 days before sample collection. The swab was collected in 3 mL medium (Deltaswab VICUM) to reduce viscosity and stored at -80ºC until use. Vero E6 cells were cultured on a cell culture flask (25 cm^2) at 1.5 x 10^6 cells overnight prior to inoculation with 1 mL of the processed sample, for 1 h at 37ºC and 5% CO_2. Afterwards, 4 mL of 2% FCS-supplemented DMEM were supplied and cells were incubated for 48 h. Supernatant was harvested, centrifuged at 200 x g for 10 min to remove cell debris and stored at -80ºC. Cells were assessed daily for cytopathic effect and the supernatant was subjected to viral RNA extraction and specific RT-qPCR using the SARS-CoV-2 UpE, RdRp and N assays (Corman et al., 2020). The virus was propagated for two passages and a virus stock was prepared collecting the supernatant from Vero E6.

Viral RNA was extracted directly from the virus stock using the Indimag Pathogen kit (Indical Biosciences) and transcribed to cDNA using the PrimeScript™ RT reagent Kit

(Takara) using oligo-dT and random hexamers, according to the manufacturer's protocol. DNA library preparation was performed using SWIFT amplicon SARS-CoV-2 panel (Swift Biosciences). Sequencing ready libraries where then loaded onto Illumina MiSeq platform and a 300bp paired-end sequencing kit. Sequence reads were quality filtered and adapter primer sequences were trimmed using trimmomatic. Amplification primer sequences were removed using cutadapt (Martin, 2011). Sequencing reads were then mapped against coronavirus reference (NC_045512.2) using bowtie2 tool (Langmead, B. and Salzberg, S, 2012). Consensus genomic sequence was called from the resulting alignment at a 18x1800x879 average coverage using samtools (Li et al., 2009). Genomic sequence was deposited at GISAID repository (http://gisaid.org) with accession ID EPI_ISL_510689.

Pseudovirus production. HIV-1 reporter pseudoviruses expressing SARS-CoV-2 Spike protein and luciferase were generated using two plasmids. pNL4-3.Luc.R-.E- was obtained from the NIH AIDS repository. SARS-CoV-2.SctΔ19 was generated (Geneart) from the full protein sequence of SARS-CoV-2 spike with a deletion of the last 19 amino acids in C-terminal, human-codon optimized and inserted into pcDNA3.4-TOPO (Ou et al., 2020b). Spike plasmid was transfected with X-tremeGENE HP Transfection Reagent (Merck) into HEK-293T cells, and 24 hours post-transfection, cells were transfected with pNL4-3.Luc.R-.E-. Supernatants were harvested 48 hours later, filtered with 0.45 µM (Millex Millipore) and stored at -80ºC until use. Control pseudoviruses were obtained by replacing the spike plasmid by a VSV-G plasmid (kindly provided by Dr. Andrea Cimarelli). The $p24^{gag}$ content of all viruses was quantified using an ELISA (Perkin Elmer) and viruses were titrated in HEK-293T overexpressing the human ACE2.

Antivirals & compounds. The complete list of compounds used for this study and vendors are shown in Supplementary Tables. Drugs were used at concentrations ranging from 100 µM to 0.0512 nM at ⅕ serial dilutions. Plitidepsin was also assayed at concentrations ranging from 10 µM to 0.5 nM at 1/3 dilutions. Interferons were assayed at concentrations ranging from 10^4 to 0.0005 IU/ml at ⅕ serial dilutions. When two drugs were combined, each one was added at a 1:1 molar ratio at concentrations ranging from 100 µM to 0.0512 nM at ⅕ serial dilutions. In combination with other drugs, plitidepsin was also assayed at concentrations ranging from 10 µM to 0.5 nM at 1/3 dilutions.

Antiviral activity. Increasing concentrations of antiviral compounds were added to Vero E6 cells together with $10^{1.8}$ TCID50/mL of SARS-CoV-2, a concentration that achieves a 50% of cytopathic effect. Untreated non-infected cells and untreated virus-infected cells were used as negative and positive controls of infection, respectively. To detect any drug-associated cytotoxic effect, Vero E6 cells were equally cultured in the presence of increasing drug concentrations, but in the absence of virus. Cytopathic or cytotoxic effects of the virus or drugs were measured 3 days after infection, using the CellTiter-Glo luminescent cell viability assay (Promega). Luminescence was measured in a Fluoroskan Ascent FL luminometer (ThermoFisher Scientific).

IC_{50} calculation and statistical analysis. Response curves of compounds or their mixes were adjusted to a non-linear fit regression model, calculated with a four-parameter logistic curve with variable slope. Cells not exposed to the virus were used as negative controls of infection, and were set as 100% of viability to normalize data and calculate the percentage of cytopathic effect. Statistical differences from 100% were assessed with a one sample t test. All analyses and figures were generated with the GraphPad Prism v8.0b Software.

In silico drug modeling. We performed Glide docking using an in-house library of all approved drug molecules on the 3CL protease of SARS-CoV-2. For this, two different receptors were used, the 6LU7 pdb structure, after removing the covalently bound inhibitor, and a combination of two crystals from the Diamond collection (https://www.diamond.ac.uk/covid-19). Receptors were prepared with the Schrodinger's protein wizard and Glide SP docking was performed with two different hydrogen bond constraints: Glu16 and His163 (with epsilon protonation); we enforced single constraints and also attempted the combination of both. The best 20 molecules, based on Glides's docking score were selected. Top docking scores, however, did not exceed -9, indicating poor potential binding.

Pseudovirus assay. HEK-293T overexpressing the human ACE2 and TMPRSS2 were used to test antivirals at the concentrations found to be effective for SARS-CoV-2 without toxicity, which were the following: 5 μM for niclosamide; 10 μM for chloroquine, chlorpromazine, ciclesonide, MDL 28170 and fenofibrate; 20 μM for hydroxychloroquine, CA-074-Me and arbidol HCl; 25 μM for E-64d; 50 μM for

Baricitinib; 100 μM for Amantadine, NB-DNJ, 3' sialyl-lactose Na salt, Tofacitinib, and Camostat mesylate; 1000 μM for methyl-β-cyclodextrin, and 12,5 mg/ml for ATT. A constant pseudoviral titer was used to pulse cells in the presence of the drugs. 48h post-inoculation, cells were lysed with the Glo Luciferase system (Promega). Luminescence was measured with an EnSight Multimode Plate Reader (Perkin Elmer).

SARS-CoV-2 detection in the supernatant of infected cells. Viral accumulation in the supernatant of Vero E6 cells infected as described previously in the presence of increasing concentrations of the indicated antiviral compounds was measured at day 3 post-infection. The amount of SARS-CoV-2 nucleoprotein released to the supernatant was measured with an ELISA (SinoBiologicals), according to the manufacturer's protocol.

TABLES

Table 1. Compounds with antiviral activity grouped in colors depending on their IC_{50} values, expressed in μM unless otherwise indicated.

FIGURES

Figure 1. Antiviral activity of entry inhibitors against SARS-CoV-2. **A.** Antiviral activity of hydroxychloroquine and azithromycin. Cytopathic effect on Vero E6 cells exposed to a fixed concentration of SARS-CoV-2 in the presence of increasing concentrations of hydroxychloroquine, azithromycin, and their combination. Drugs were used at a concentration ranging from 0.0512 nM to 100 μM. When combined, each drug was added at the same concentration. Non-linear fit to a variable response curve from one representative experiment with two replicates is shown (red lines), excluding data from drug concentrations with associated toxicity. The particular IC_{50} value of this graph is indicated. Cytotoxic effect on Vero E6 cells exposed to increasing concentrations of drugs in the absence of virus is also shown (grey lines). **B.** Cytopathic effect on Vero E6 cells exposed to a fixed concentration of SARS-CoV-2 in the presence of increasing concentrations of amantadine, a clathrin-mediated endocytosis inhibitor, E-64d, a pan-cathepsin inhibitor acting downstream once viruses are internalized in endosomes, NB-DNJ, an inhibitor of ganglioside biosynthesis and methyl-β-cyclodextrin, a cholesterol-depleting agent. All drugs were used at a concentration ranging from 0.0512 nM to 100 μM aside from methyl-β-cyclodextrin, which was used 10 times more concentrated. Non-linear fit to a variable response curve from one experiment with two replicates is shown (red lines). Cytotoxic effect on Vero E6 cells exposed to increasing concentrations of drugs in the absence of virus is also shown (grey lines). **C.** Cytopathic effect on Vero E6 cells exposed to a fixed concentration of SARS-CoV-2 in the presence of increasing concentrations of camostat, a TMPRSS2 inhibitor, and ATT, an alfa-1 antyitrypsin, a broad cellular protease inhibitor, as described in **A**. **D.** Effect of entry inhibitors on luciferase expression of reporter lentiviruses pseudotyped with SARS-CoV-2 Spike in ACE2 expressing HEK-293T cells. Values are normalized to luciferase expression by mock-treated cells set at 100%. Mean and s.e.m. from two experiments with two replicates. Cells were exposed to fixed amounts of SARS-CoV-2 Spike lentiviruses in the presence of a non-toxic constant concentration of the drugs tested on Vero E6. Statistical

deviations from 100% were assessed with a one sample t test. **E.** Comparison of entry inhibitors blocking viral endocytosis, such as chloroquine, with inhibitors blocking serine protease TMPRSS2 expressed on the cellular membrane, such as camostat, on different cell lines. ACE2 expressing HEK-293T cells transfected or not with TMPRSS2 were exposed to SARS-CoV-2 Spike lentiviruses as described in **B**. Values are normalized to luciferase expression by mock-treated cells set at 100%. Mean and s.e.m. from at least two representative experiments with two replicates. Statistical deviations from 100% were assessed with a one sample t test.

Figure 2. Antiviral activity of post-entry inhibitors. **A.** Cytopathic effect on Vero E6 cells exposed to a fixed concentration of SARS-CoV-2 in the presence of increasing concentrations of Remdesivir. Drug was used at a concentration ranging from 0.0512 nM to 100 µM. Non-linear fit to a variable response curve from one representative experiment with two replicates is shown (red lines), excluding data from drug concentrations with associated toxicity. The particular IC_{50} value of this graph is indicated. Cytotoxic effect on Vero E6 cells exposed to increasing concentrations of drugs in the absence of virus is also shown (grey lines). **B.** Cytopathic effect on Vero E6 cells exposed to a fixed concentration of SARS-CoV-2 in the presence of increasing concentrations of remdesivir and its combination with hydroxychloroquine, as detailed in **A**. Drugs in combination were used at a concentration ranging from 0.0512 nM to 100 µM (left panel). Alternatively, remdesivir was used at a concentration ranging from 0.0512 nM to 100 µM at the fixed indicated concentrations of hydroxychloroquine (right panel). **C.** Cytopathic effect on Vero E6 cells exposed to a fixed concentration of SARS-CoV-2 in the presence of increasing concentrations of protease inhibitors against HIV-1. Nelfinavir mesylate hydrate was the only drug with activity. Inhibitors were used at a concentration ranging from 0.0512 nM to 100 µM. The particular IC_{50} value of this graph is indicated **D.** Cytopathic effect on Vero E6 cells exposed to a fixed concentration of SARS-CoV-2 in the presence of increasing concentrations of plitidepsin and its combinations with hydroxychloroquine and remdesivir. When combined, each drug was added at the same concentration. Drugs were used at a concentration ranging from 0.5 nM to 10 µM. The particular IC_{50} value of these graphs is indicated.

Figure 3. Antiviral activity of inhibitors with unknown mechanism of action. **A.** Cytopathic effect on Vero E6 cells exposed to a fixed concentration of SARS-CoV-2 in

the presence of increasing concentrations of Itraconazole. Drug was used at a concentration ranging from 0.0512 nM to 100 μM . Non-linear fit to a variable response curve from one representative experiment with two replicates is shown (red lines), excluding data from drug concentrations with associated toxicity. The particular IC_{50} value of this graph is indicated. Cytotoxic effect on Vero E6 cells exposed to increasing concentrations of drugs in the absence of virus is also shown (grey lines). **B.** Cytopathic effect on Vero E6 cells exposed to a fixed concentration of SARS-CoV-2 in the presence of increasing concentrations of Fenofibrate, as detailed in **A**. **C**. Effect of fenofibrate on the entry of luciferase expressing lentiviruses pseudotyped with SARS-CoV-2 Spike in ACE2-expressing HEK-293T cells. Values are normalized to luciferase expression by mock-treated cells set at 100%. Mean and s.e.m. from two experiments with two replicates. Statistical deviations from 100% were assessed with a one sample t test. **D**. Cytopathic effect on Vero E6 cells exposed to a fixed concentration of SARS-CoV-2 in the presence of increasing concentrations of MDL 28170, as detailed in **A**. **E**. Comparison of MDL 28170 activity with entry inhibitors blocking viral endocytosis, such as chloroquine and E-64d, and inhibitors blocking serine protease TMPRSS2, such as camostat. ACE2 expressing HEK-293T cells transfected or not with TMPRSS2 were exposed to SARS-CoV-2 Spike lentiviruses in the presence of these compounds. Values are normalized to luciferase expression by mock-treated cells set at 100%. Mean and s.e.m. from at least two experiments with two replicates. Statistical deviations from 100% were assessed with a one sample t test.

Figure 4. Decreased release of SARS-CoV-2 in the presence of inhibitors with antiviral activity. **A.** Viral release to the supernatant in the presence of the indicated compounds added at increasing concentrations 3 days post-infection of Vero E6 cells. SARS-CoV-2 nucleoprotein was detected with an ELISA at concentrations were drugs were nontoxic. Mean and s.e.m. from two experiments. **B.** Viral release to the supernatant in the presence of the indicated interferons as described in A. Mean and s.e.m. from one experiment.

SUPPLEMENTARY TABLES

Supp. Table 1. Antiviral activity of potential entry inhibitors tested against SARS-CoV-2. NA; Not active. IC_{50} values are reported in μM unless otherwise indicated.

Supp. Table 2. Antiviral activity of potential inhibitors against SARS-CoV-2 tested in combination. NA; Not active.

Supp. Table 3. Antiviral activity of potential post-entry inhibitors against SARS-CoV-2. NA; Not active. IC_{50} values are reported in μM unless otherwise indicated.

Supp. Table 4. Antiviral activity of potential inhibitors against SARS-CoV-2 with predicted capacity to block SARS-CoV-2 viral protease. NA; Not active.

Supp. Table 5. Antiviral activity of potential inhibitors against SARS-CoV-2 with unknown mechanism of action. NA; Not active.

SUPPLEMENTARY FIGURES

Supplementary Figure 1. No antiviral activity of HIV-1 reverse transcriptase inhibitors. Cytopathic effect on Vero E6 cells exposed to a fixed concentration of SARS-CoV-2 in the presence of increasing concentrations of HIV-1 reverse transcriptase inhibitors. Drugs were used at a concentration ranging from 0.0512 nM to 100 μM. Non-linear fit to a variable response curve from one experiment with two replicates is shown (red lines). Cytotoxic effect on Vero E6 cells exposed to increasing concentrations of drugs in the absence of virus is also shown (grey lines).

Supplementary Figure 2. Antiviral activity of NPO calpain and cathepsin inhibitors. Cytopathic effect on Vero E6 cells exposed to a fixed concentration of SARS-CoV-2 in the presence of increasing concentrations of calpain and cathepsin inhibitors NPO. Drugs were used at a concentration ranging from 0.0512 nM to 100 μM. Non-linear fit to a variable response curve from one experiment with two replicates is shown (red lines). Cytotoxic effect on Vero E6 cells exposed to increasing concentrations of drugs in the absence of virus is also shown (grey lines).

BIBLIOGRAPHY

Arshad, S., Kilgore, P., Chaudhry, Z.S., Jacobsen, G., Wang, D.D., Huitsing, K., Brar, I., Alangaden, G.J., Ramesh, M.S., McKinnon, J.E., et al. (2020). Treatment with hydroxychloroquine, azithromycin, and combination in patients hospitalized with COVID-19. Int. J. Infect. Dis. *97*, 396–403.

Beigel, J.H., Tomashek, K.M., Dodd, L.E., Mehta, A.K., Zingman, B.S., Kalil, A.C., Hohmann, E., Chu, H.Y., Luetkemeyer, A., Kline, S., et al. (2020). Remdesivir for the Treatment of Covid-19 — Preliminary Report. N. Engl. J. Med. NEJMoa2007764.

Boulware, D.R., Pullen, M.F., Bangdiwala, A.S., Pastick, K.A., Lofgren, S.M., Okafor, E.C., Skipper, C.P., Nascene, A.A., Nicol, M.R., Abassi, M., et al. (2020). A Randomized Trial of Hydroxychloroquine as Postexposure Prophylaxis for Covid-19. N. Engl. J. Med. NEJMoa2016638.

Caly, L., Druce, J.D., Catton, M.G., Jans, D.A., and Wagstaff, K.M. (2020). The FDA-approved Drug Ivermectin inhibits the replication of SARS-CoV-2 in vitro. Antiviral Res. 104787.

Cavalcanti, A.B., Zampieri, F.G., Rosa, R.G., Azevedo, L.C.P., Veiga, V.C., Avezum, A., Damiani, L.P., Marcadenti, A., Kawano-Dourado, L., Lisboa, T., et al. (2020). Hydroxychloroquine with or without Azithromycin in Mild-to-Moderate Covid-19. N. Engl. J. Med. NEJMoa2019014.

Chen, N., Zhou, M., Dong, X., Qu, J., Gong, F., Han, Y., Qiu, Y., Wang, J., Liu, Y., Wei, Y., et al. (2020). Epidemiological and clinical characteristics of 99 cases of 2019 novel coronavirus pneumonia in Wuhan, China: a descriptive study. The Lancet S0140673620302117.

Corman, V.M., Landt, O., Kaiser, M., Molenkamp, R., Meijer, A., Chu, D.K., Bleicker, T., Brünink, S., Schneider, J., Schmidt, M.L., et al. (2020). Detection of 2019 novel coronavirus (2019-nCoV) by real-time RT-PCR. Eurosurveillance *25*.

Elfiky, A.A. (2020). Ribavirin, Remdesivir, Sofosbuvir, Galidesivir, and Tenofovir against SARS-CoV-2 RNA dependent RNA polymerase (RdRp): A molecular docking study. Life Sci. *253*, 117592.

Emeny, J.M., and Morgan, M.J. (1979). Regulation of the Interferon System: Evidence that Vero Cells have a Genetic Defect in Interferon Production. J. Gen. Virol. *43*, 247–252.

Fantini, J., Di Scala, C., Chahinian, H., and Yahi, N. (2020). Structural and molecular modelling studies reveal a new mechanism of action of chloroquine and hydroxychloroquine against SARS-CoV-2 infection. Int. J. Antimicrob. Agents 105960.

Gassen, N.C., Papies, J., Bajaj, T., Dethloff, F., Emanuel, J., Weckmann, K., Heinz, D.E., Heinemann, N., Lennarz, M., Richter, A., et al. (2020). Analysis of SARS-CoV-2-controlled autophagy reveals spermidine, MK-2206, and niclosamide as putative antiviral therapeutics (Microbiology).

Gautret, P., Lagier, J.-C., Parola, P., Hoang, V.T., Meddeb, L., Mailhe, M., Doudier, B., Courjon, J., Giordanengo, V., Vieira, V.E., et al. (2020). Hydroxychloroquine and azithromycin as a treatment of COVID-19: results of an open-label non-randomized clinical trial. Int. J. Antimicrob. Agents 105949.

Gielen, V., Johnston, S.L., and Edwards, M.R. (2010). Azithromycin induces anti-viral responses in bronchial epithelial cells. Eur. Respir. J. *36*, 646–654.

Grein, J., Ohmagari, N., Shin, D., Diaz, G., Asperges, E., Castagna, A., Feldt, T., Green, G., Green, M.L., Lescure, F.-X., et al. (2020). Compassionate Use of Remdesivir for Patients with Severe Covid-19. N. Engl. J. Med. NEJMoa2007016.

Hadjadj, J., Yatim, N., Barnabei, L., Corneau, A., Boussier, J., Smith, N., Péré, H., Charbit, B., Bondet, V., Chenevier-Gobeaux, C., et al. (2020). Impaired type I interferon activity and inflammatory responses in severe COVID-19 patients. Science eabc6027.
Hanley, B., Naresh, K.N., Roufosse, C., Nicholson, A.G., Weir, J., Cooke, G.S., Thursz, M., Manousou, P., Corbett, R., Goldin, R., et al. (2020). Histopathological findings and viral tropism in UK patients with severe fatal COVID-19: a post-mortem study. Lancet Microbe S2666524720301154.
Haviernik, J., Štefánik, M., Fojtíková, M., Kali, S., Tordo, N., Rudolf, I., Hubálek, Z., Eyer, L., and Ruzek, D. (2018). Arbidol (Umifenovir): A Broad-Spectrum Antiviral Drug That Inhibits Medically Important Arthropod-Borne Flaviviruses. Viruses *10*, 184.
Hoffmann, M. SARS-CoV-2 Cell Entry Depends on ACE2 and TMPRSS2 and Is Blocked by a Clinically Proven Protease Inhibitor. 19.
Hoffmann, M., Kleine-Weber, H., Krueger, N., Mueller, M.A., Drosten, C., and Poehlmann, S. (2020). The novel coronavirus 2019 (2019-nCoV) uses the SARS-coronavirus receptor ACE2 and the cellular protease TMPRSS2 for entry into target cells (Molecular Biology).
Hu, T.Y., Frieman, M., and Wolfram, J. (2020). Insights from nanomedicine into chloroquine efficacy against COVID-19. Nat. Nanotechnol.
Jeon, S., Ko, M., Lee, J., Choi, I., Byun, S.Y., Park, S., Shum, D., and Kim, S. (2020). Identification of antiviral drug candidates against SARS-CoV-2 from FDA-approved drugs (Microbiology).
Langmead, B., and Salzberg, S (2012). Fast gapped-read alignment with Bowtie 2. Nat Methods *9*, 357–359.
Li (2020). An exploratory randomized controlled study on the efficacy and safety of lopinavir/ritonavir or arbidol treating adult patients hospitalized with mild/moderate COVID-19 (ELACOI). MedRxiv 33.
Li, H., Handsaker, B., Wysoker, A., Fennell, T., Ruan, J., Homer, N., Marth, G., Abecasis, G., Durbin, R., and 1000 Genome Project Data Processing Subgroup (2009). The Sequence Alignment/Map format and SAMtools. Bioinformatics *25*, 2078–2079.
Liu, J., Cao, R., Xu, M., Wang, X., Zhang, H., Hu, H., Li, Y., Hu, Z., Zhong, W., and Wang, M. (2020). Hydroxychloroquine, a less toxic derivative of chloroquine, is effective in inhibiting SARS-CoV-2 infection in vitro. Cell Discov. *6*, 16.
Lu, Y., Liu, D.X., and Tam, J.P. (2008). Lipid rafts are involved in SARS-CoV entry into Vero E6 cells. Biochem. Biophys. Res. Commun. *369*, 344–349.
Maisonnasse, P., Guedj, J., Contreras, V., Behillil, S., Solas, C., Marlin, R., Naninck, T., Pizzorno, A., Lemaitre, J., Gonçalves, A., et al. (2020). Hydroxychloroquine use against SARS-CoV-2 infection in non-human primates. Nature.
Martin, M. (2011). Cutadapt Removes Adapter Sequences from High-Throughput Sequencing Reads. EMBnet.Journal *17*, 310.
Mingo, R.M., Simmons, J.A., Shoemaker, C.J., Nelson, E.A., Schornberg, K.L., D'Souza, R.S., Casanova, J.E., and White, J.M. (2015). Ebola Virus and Severe Acute Respiratory Syndrome Coronavirus Display Late Cell Entry Kinetics: Evidence that Transport to NPC1 $^{+}$ Endolysosomes Is a Rate-Defining Step. J. Virol. *89*, 2931–2943.
Monteil, V., Kwon, H., Prado, P., Hagelkrüys, A., Wimmer, R.A., Stahl, M., Leopoldi, A., Garreta, E., Romero, J.P., Wirnsberger, G., et al. Inhibition of SARS-CoV-2 infections in engineered human tissues using clinical-grade soluble human ACE2. 29.
Ou, T., Mou, H., Zhang, L., Ojha, A., Choe, H., and Farzan, M. (2020a). Hydroxychloroquine-mediated inhibition of SARS-CoV-2 entry is attenuated by TMPRSS2 (Microbiology).
Ou, X., Liu, Y., Lei, X., Li, P., Mi, D., Ren, L., Guo, L., Guo, R., Chen, T., Hu, J., et al.

(2020b). Characterization of spike glycoprotein of SARS-CoV-2 on virus entry and its immune cross-reactivity with SARS-CoV. Nat. Commun. *11*, 1620.
Pan, H et al. WHO Solidarity trial consortium. (2020). Repurposed antiviral drugs for COVID-19 –interim WHO SOLIDARITY trial results. medRxiv 15 October v.
Phonphok, Y., and Rosenthal, K.S. (1991). Stabilization of clathrin coated vesicles by amantadine, tromantadine and other hydrophobic amines. FEBS Lett. *281*, 188–190.
Richardson, P., Griffin, I., Tucker, C., Smith, D., Oechsle, O., Phelan, A., and Stebbing, J. (2020). Baricitinib as potential treatment for 2019-nCoV acute respiratory disease. The Lancet *395*, e30–e31.
Riva, L., Yuan, S., Yin, X., Martin-Sancho, L., Matsunaga, N., Pache, L., Burgstaller-Muehlbacher, S., De Jesus, P.D., Teriete, P., Hull, M.V., et al. (2020). Discovery of SARS-CoV-2 antiviral drugs through large-scale compound repurposing. Nature.
Rosenke, K., Jarvis, M.A., Feldmann, F., Schwarz, B., Okumura, A., Lovaglio, J., Saturday, G., Hanley, P.W., Meade-White, K., Williamson, B.N., et al. (2020). Hydroxychloroquine Proves Ineffective in Hamsters and Macaques Infected with SARS-CoV-2 (Pharmacology and Toxicology).
Schneider, M., Ackermann, K., Stuart, M., Wex, C., Protzer, U., Schätzl, H.M., and Gilch, S. (2012). Severe Acute Respiratory Syndrome Coronavirus Replication Is Severely Impaired by MG132 due to Proteasome-Independent Inhibition of M-Calpain. J. Virol. *86*, 10112–10122.
Simmons, G., Gosalia, D.N., Rennekamp, A.J., Reeves, J.D., Diamond, S.L., and Bates, P. (2005). Inhibitors of cathepsin L prevent severe acute respiratory syndrome coronavirus entry. Proc. Natl. Acad. Sci. *102*, 11876–11881.
Song, Z., Xu, Y., Bao, L., Zhang, L., Yu, P., Qu, Y., Zhu, H., Zhao, W., Han, Y., and Qin, C. (2019). From SARS to MERS, Thrusting Coronaviruses into the Spotlight. Viruses *11*, 59.
Stebbing, J., Phelan, A., Griffin, I., Tucker, C., Oechsle, O., Smith, D., and Richardson, P. (2020). COVID-19: combining antiviral and anti-inflammatory treatments. Lancet Infect. Dis. *20*, 400–402.
Tu, Y.-F., Chien, C.-S., Yarmishyn, A.A., Lin, Y.-Y., Luo, Y.-H., Lin, Y.-T., Lai, W.-Y., Yang, D.-M., Chou, S.-J., Yang, Y.-P., et al. (2020). A Review of SARS-CoV-2 and the Ongoing Clinical Trials. Int. J. Mol. Sci. *21*, 2657.
Wang, L.H., Rothberg, K.G., and Anderson, R.G. (1993). Mis-assembly of clathrin lattices on endosomes reveals a regulatory switch for coated pit formation. J. Cell Biol. *123*, 1107–1117.
Wang, M., Cao, R., Zhang, L., Yang, X., Liu, J., Xu, M., Shi, Z., Hu, Z., Zhong, W., and Xiao, G. (2020). Remdesivir and chloroquine effectively inhibit the recently emerged novel coronavirus (2019-nCoV) in vitro. Cell Res. *30*, 269–271.
WHO (2020). "Solidarity" clinical trial for COVID-19 treatments.
Williamson, B., Feldmann, F., Schwarz, B., Meade-White, K., Porter, D., Schulz, J., van Doremalen, N., Leighton, I., Yinda, C.K., Perez-Perez, L., et al. (2020). Clinical benefit of remdesivir in rhesus macaques infected with SARS-CoV-2 (Microbiology).
Wu, C., Liu, Y., Yang, Y., Zhang, P., Zhong, W., Wang, Y., Wang, Q., Xu, Y., Li, M., Li, X., et al. (2020). Analysis of therapeutic targets for SARS-CoV-2 and discovery of potential drugs by computational methods. Acta Pharm. Sin. B *10*, 766–788.
Zhou, Y., and Simmons, G. (2012). Development of novel entry inhibitors targeting emerging viruses. Expert Rev. Anti Infect. Ther. *10*, 1129–1138.

ACKNOWLEDGEMENTS

We are grateful to patients at the Hospital Germans Trias i Pujol that donated their samples for research. For his excellent assistance and advice, we thank Jordi Puig from Fundació Lluita contra la SIDA. We are most grateful to Lidia Ruiz and the Clinical Sample Management Team of IrsiCaixa for their outstanding sample processing and management, and to M. Pilar Armengol and the translational genomics platform team at the Institut de Recerca Germans Trias i Pujol. We truly thank B. Trinité for generating the Spike expression plasmid construct used in this study. We thank Pharma Mar, Rubió Laboratories, Janssen and Drs. Cabrera and Ballana form IrsiCaixa; Pascual-Figal, Lax and Asensio-Lopez MC from "Instituto de Investigación Biosanitaria IMIB-Arrixaca" of Murcia; and Fernández-Real and Barretina from the "Institut d'Investigació Biomèdica de Girona Dr. Josep Trueta" for providing some of the reagents tested.

FINANCIAL SUPPORT

The research of CBIG consortium (constituted by IRTA-CReSA, BSC, & IrsiCaixa) is supported by Grifols pharmaceutical. The authors also acknowledge the crowdfunding initiative #Yomecorono (https://www.yomecorono.com). JS, JVA and NIU have non-restrictive funding from Pharma Mar to study the antiviral effect of plitidepsin. The funders had no role in study design, data collection and analysis, decision to publish, or preparation of the manuscript.

COMPETING INTEREST

A patent application based on this work has been filed (EP20382821.5). The authors declare that no other competing financial interests exist.

AUTHOR CONTRIBUTION

Conceived and designed the experiments: JR, JMB, DPZ, JS, BC, JVA, NIU

Performed in silico drug modeling: VG

Performed experiments: JR, JMB, DPZ, MNJ, IE, VG, JVA, NIU

Contributed with critical reagents: CQ

Analyzed and interpreted the data: JR, JMB, DPZ, MNJ, RP, LM, CQ, IE, AV, VG, JC, JB, JS, BC, JVA, NIU

Wrote the paper: JR, JVA, NIU

DATA AVAILABILITY Data is available from corresponding authors upon reasonable request.

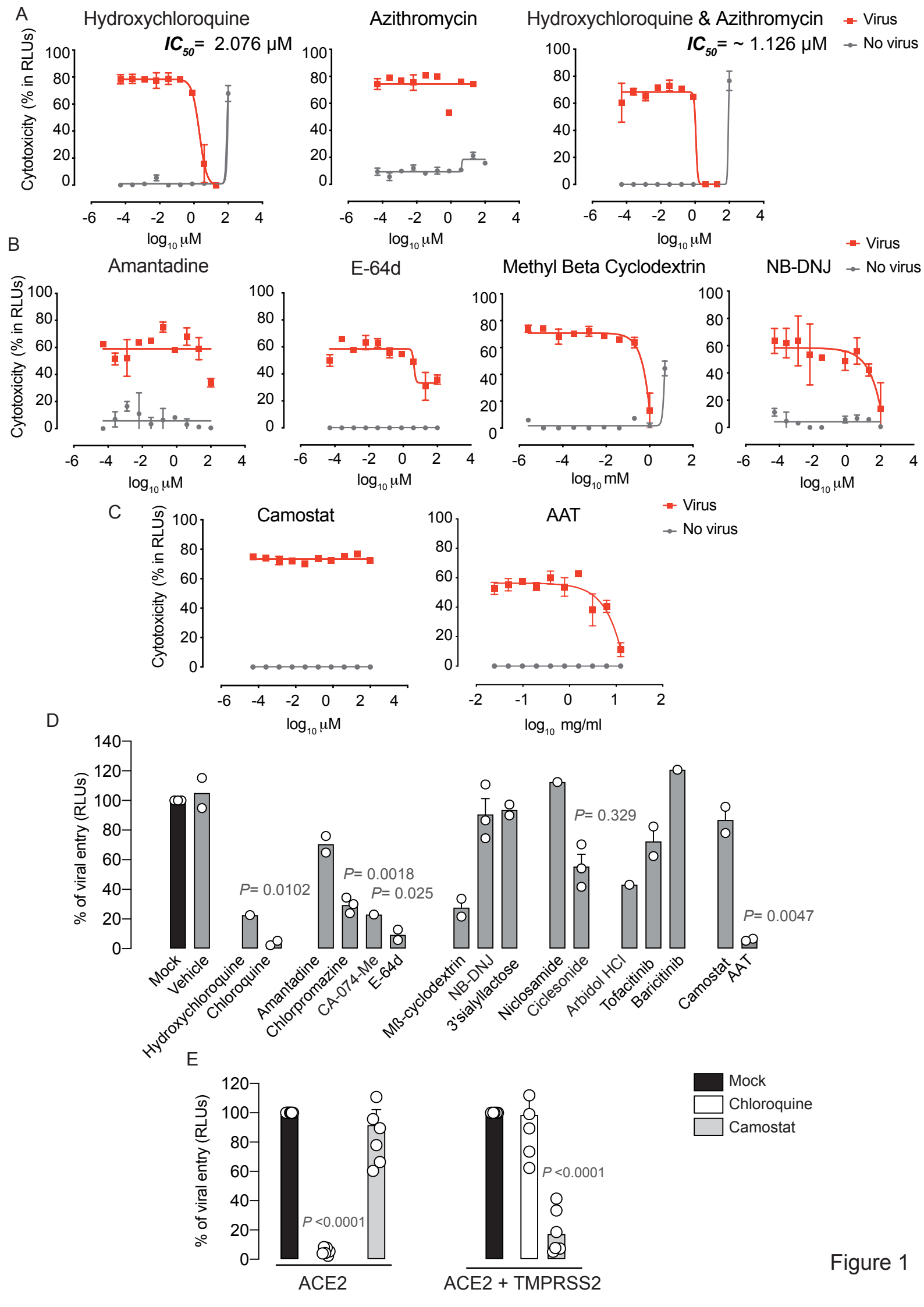
A
Hydroxychloroquine
IC50= 2.076 μM
Azithromycin
Hydroxychloroquine & Azithromycin
IC50= ~ 1.126 μM
Virus
No virus
Cytotoxicity (% in RLUs)
log10 μM
B
Amantadine
E-64d
Methyl Beta Cyclodextrin
NB-DNJ
log10 mM
C
Camostat
AAT
log10 mg/ml
D
% of viral entry (RLUs)
P= 0.0102
P= 0.0018
P= 0.025
P= 0.329
P= 0.0047
Mock
Vehicle
Hydroxychloroquine
Chloroquine
Amantadine
Chlorpromazine
CA-074-Me
E-64d
Mß-cyclodextrin
NB-DNJ
3'sialyllactose
Niclosamide
Ciclesonide
Arbidol HCl
Tofacitinib
Baricitinib
Camostat
AAT
E
Mock
Chloroquine
Camostat
P <0.0001
P <0.0001
ACE2
ACE2 + TMPRSS2

Figure 1

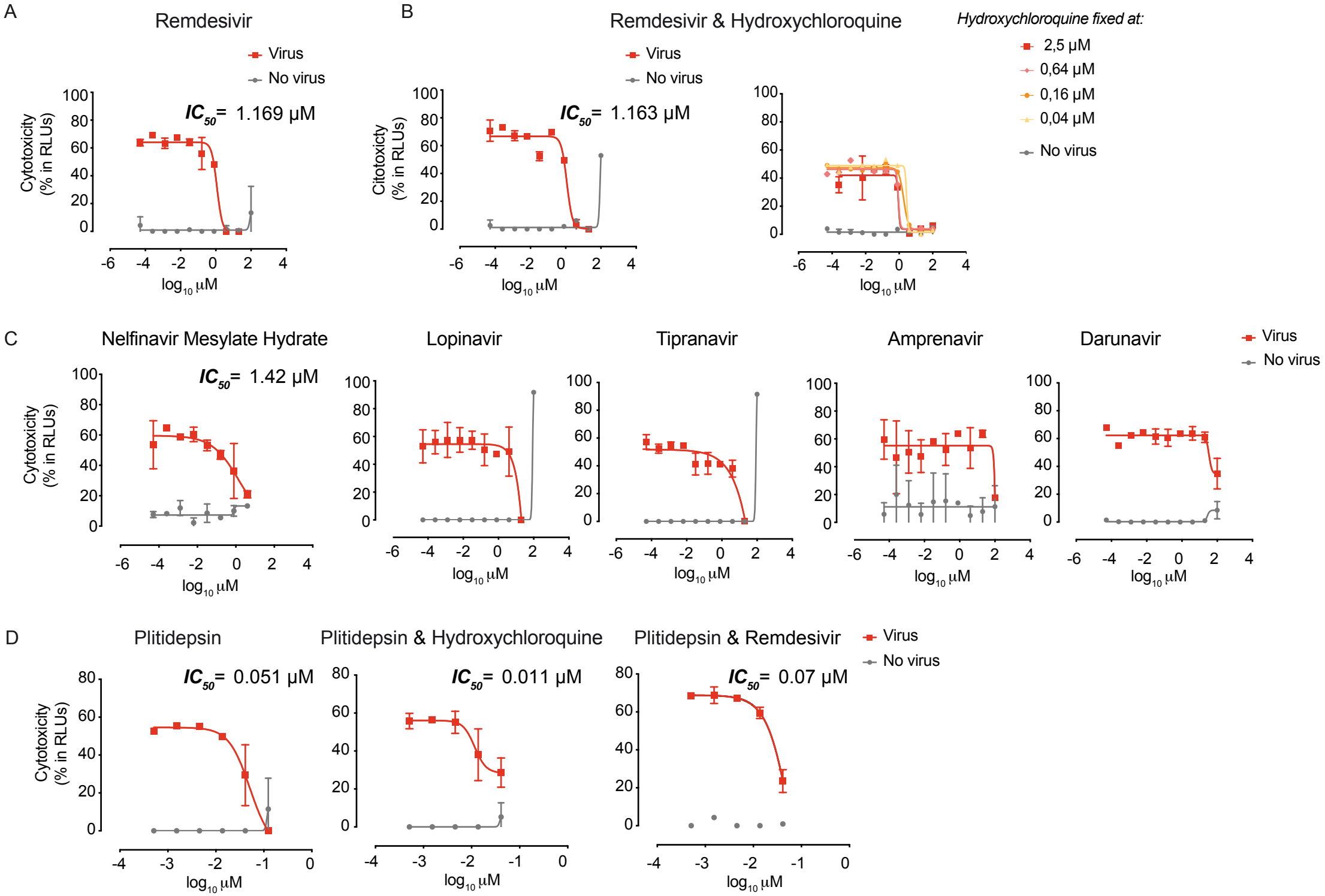
A
Remdesivir
Virus
No virus
IC50= 1.169 µM
Cytotoxicity (% in RLUs)
log10 µM
B
Remdesivir & Hydroxychloroquine
Virus
No virus
IC50= 1.163 µM
Citotoxicity (% in RLUs)
log10 µM
Hydroxychloroquine fixed at:
2,5 µM
0,64 µM
0,16 µM
0,04 µM
No virus
C
Nelfinavir Mesylate Hydrate
IC50= 1.42 µM
Lopinavir
Tipranavir
Amprenavir
Darunavir
Virus
No virus
Cytotoxicity (% in RLUs)
log10 µM
D
Plitidepsin
IC50= 0.051 µM
Plitidepsin & Hydroxychloroquine
IC50= 0.011 µM
Plitidepsin & Remdesivir
IC50= 0.07 µM
Virus
No virus
Cytotoxicity (% in RLUs)
log10 µM

Figure 2

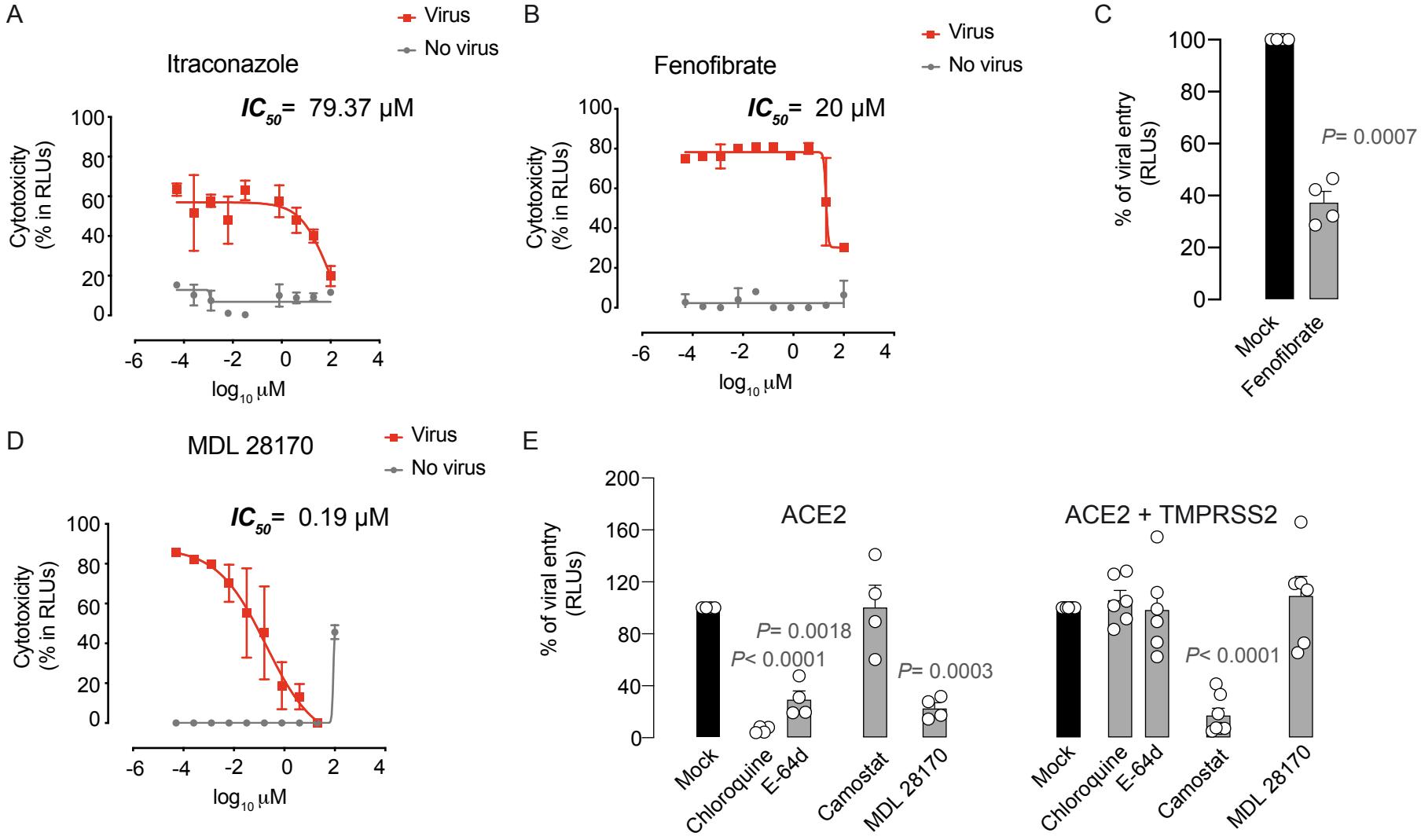
A
Virus
No virus
Itraconazole
IC50= 79.37 μM
Cytotoxicity (% in RLUs)
log10 μM
B
Virus
No virus
Fenofibrate
IC50= 20 μM
Cytotoxicity (% in RLUs)
log10 μM
C
% of viral entry (RLUs)
P= 0.0007
Mock
Fenofibrate
D
MDL 28170
Virus
No virus
IC50= 0.19 μM
Cytotoxicity (% in RLUs)
log10 μM
E
% of viral entry (RLUs)
ACE2
P= 0.0018
P< 0.0001
P= 0.0003
Mock
Chloroquine
E-64d
Camostat
MDL 28170
ACE2 + TMPRSS2
P< 0.0001
Mock
Chloroquine
E-64d
Camostat
MDL 28170

Figure 3

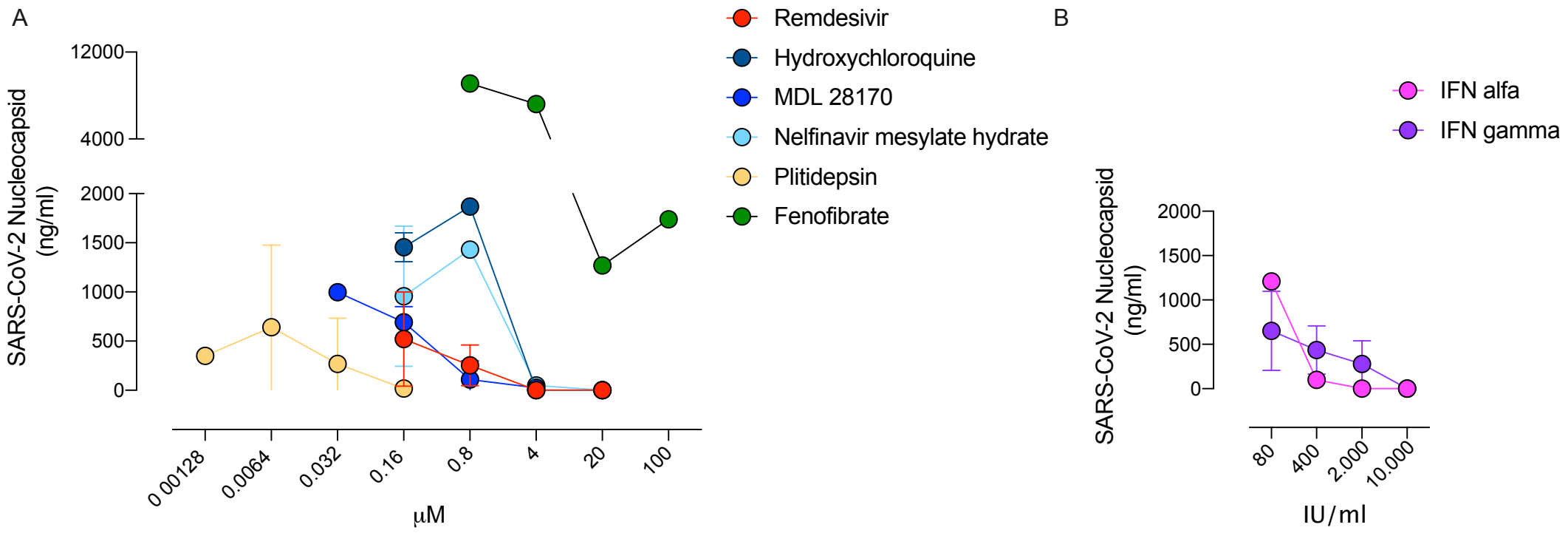
A
SARS-CoV-2 Nucleocapsid (ng/ml)
12000
4000
2000
1500
1000
500
0
0.00128
0.0064
0.032
0.16
0.8
4
20
100
µM
Remdesivir
Hydroxychloroquine
MDL 28170
Nelfinavir mesylate hydrate
Plitidepsin
Fenofibrate
B
IFN alfa
IFN gamma
SARS-CoV-2 Nucleocapsid (ng/ml)
2000
1500
1000
500
0
80
400
2.000
10.000
IU/ml

Figure 4

	DRUG	IC_{50} / CC_{50} µM (Mean +/-SD)	Mode of Action	Previous Clinical Use	Vendor Origen
nM	Plitidepsin	0.06 +/- 0.02 / > 0.1	Targets eukaryotic Elongation Factor 1A2 (eEF1A2)	Multiple myeloma	PharmaMar
	MDL 28170	0.14 +/- 0.06 / > 87	Calpain III inhibitor & Cathepsin B	*Pre-Clinical*	Merck
	NPO-2142; -2143 & -2260	~ 0.54 / Non toxic	Calpain & Cathepsin inhibitors	*Pre-Clinical*	Landsteiner Genmed
< 25 µM or 10^2 IU/mL	Remdesivir	2.16 +/-4.1 / > 85	RNA Polymerase inhibitor	Ebola Virus	Cayman Chemical
	Hydroxycloroquine	10.9 +/- 11.3 / > 96	Clathrin-mediated endocitosys or pH-dependent viral fusion inhibitor	Malaria	Laboratorios Rubio
	Nelfinavir mesylate hydrate	*Not calculated, but active < 10* / > 25	Protease inhibitor	HIV-1	Sigma Aldrich
	Chloroquine	3.86 / > 25	Clathrin-mediated endocitosys or pH-dependent viral fusion inhibitor	Malaria	Sigma Aldrich
	Interferon 2 alfa	8.1+/-0.7 x10^2 IU/mL / Non toxic	INF stimulated antiviral proteins	Hepatitis & HIV-1	Sigma-Aldrich
	Interferon gamma	11.2 x10^2 IU/mL / Non toxic	INF stimulated antiviral proteins	Granulomatous disease	Sigma-Aldrich
	Fenofibrate	19.8+/- 8 / Non Toxic	Activates PPARα	Dyslipidemia	Lacer
< 50 µM	Lopinavir	*Not calculated, but active at 20* / > 87	Protease inhibitor	HIV-1	Abbot
	Tipranavir	*Not calculated, but active at 20* / > 70	Protease inhibitor	HIV-1	HPLC
< 100 µM	Itraconazole	79.37 / Non toxic	Inhibits OSBP, which produces the membrane-bound viral replication organelles	Fungus	Janssen
	Amprenavir	*Not calculated, but active at 100/* Non toxic	Protease inhibitor	HIV-1	GSK
	NB-DNJ	*Not calculated, but active at 100* / Non toxic	ceramide-glucosyltransferase and β-glucosidase 2 inhibitor	Gaucher disease & Juvenile Sandhoff disease	Calbiochem
> 100 µM	Darunavir	*Not calculated, but partially active at 100* / Non toxic	Protease inhibitor	HIV-1	Sigma Aldrich
	Favipiravir	*Not calculated, but partially active at 100* / Non toxic	RNA polymerase inhibitor	Flavivirus, Arenavirus, Bunyavirus, Alphavirus	Quimigen
	Amantadine	*Not calculated, but partially active at 100* / Non toxic	Clathrin-mediated endocytosis inhibitor	Parkinson & influenza A	Sigma Aldrich
	E-64d	*Not calculated, but partially active at 100* / Non toxic	Cathepsin inhibitor B/L	*Pre-Clinical*	Sigma Aldrich
	Alfa-1 Antitrypsin	*Not calculated, but partially active at 12.5 mg/ml* / Non toxic	Cellular protease inhibitor	Alfa-1 antitrypsin deficiency	Grifols

Table 1

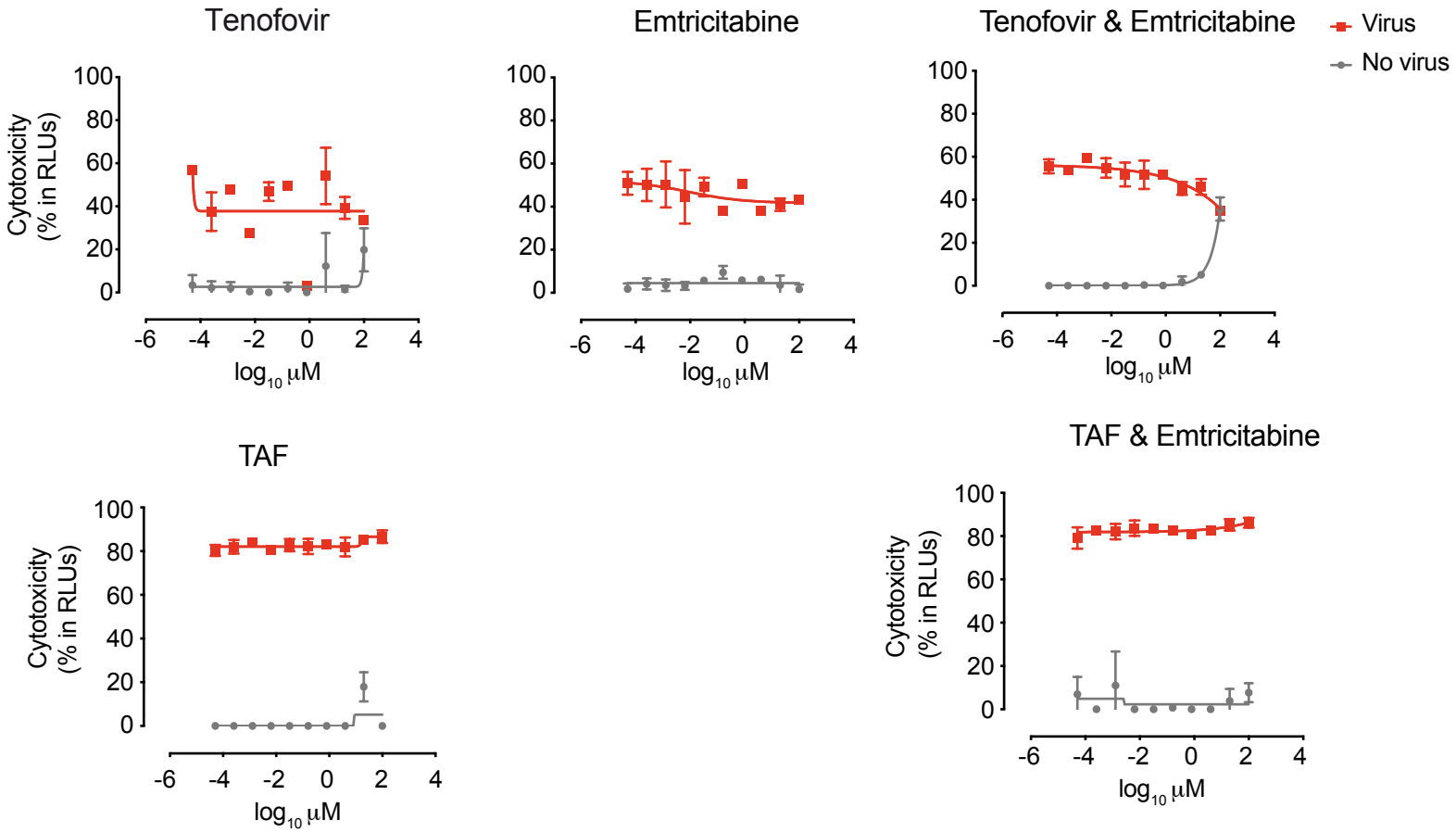

Supplementary Figure 1

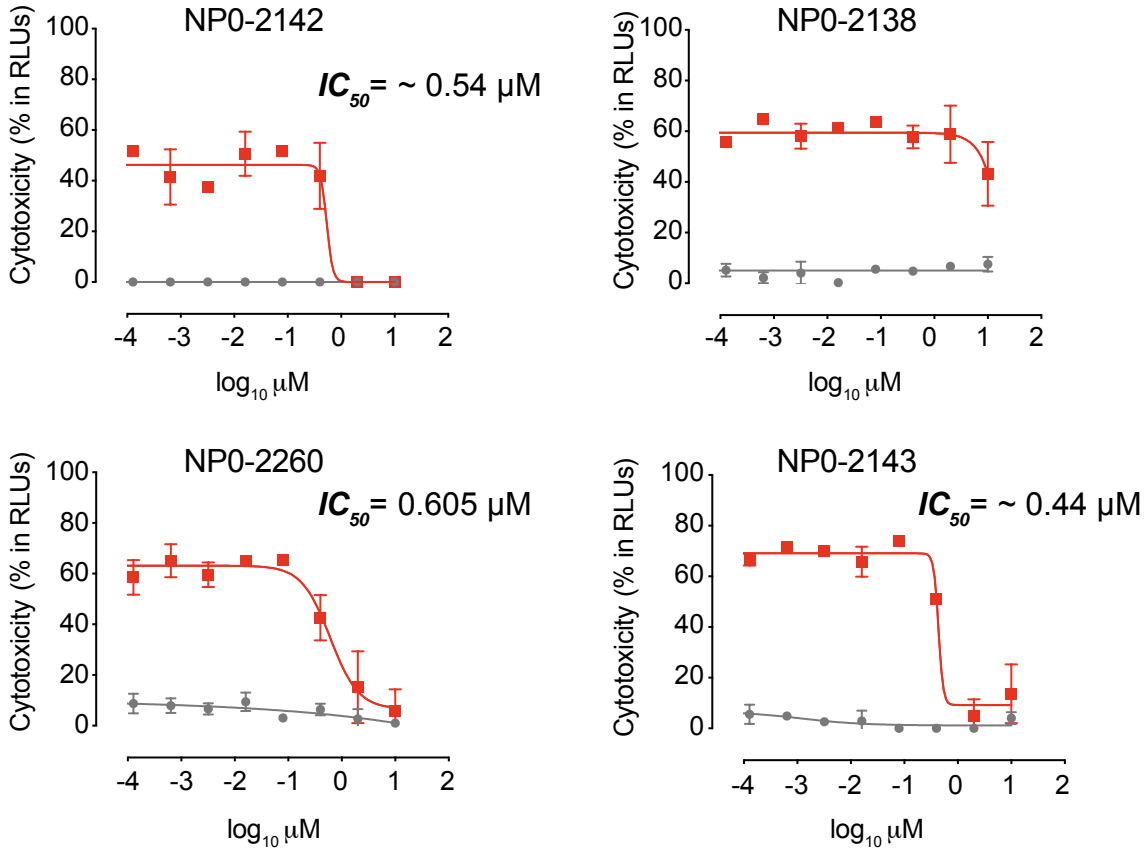

Supplementary Figure 2

ACTIVITY	DRUG	IC_{50} / CC_{50} µM (Mean +/-SD)	Mode of Action	Previous Clinical Use	Vendor Origen
ENTRY	Hydroxychloroquine	9.3 +/- 11.1 / > 80	Clathrin-mediated endocitosys or pH-dependent viral fusion inhibitor	Malaria	Laboratorios Rubió
	Chloroquine	3.9 / > 25			Sigma Aldrich
	Amantadine	*Not calculated, but partialy active at 100 /* Non toxic	Clathrin-mediated endocitosys inhibitor	Parkinson & influenza A	Sigma Aldrich
	Chlorpromazine (Largactil)	Not Active / > 18	Clathrin-mediated endocitosys inhibitor	Antipsychotic	Sanofi
	CA-074-Me	Not Active / > 34	Cathepsin inhibitor B	*Pre-Clinical*	Sigma Aldrich
	E-64d	*Not calculated, but partialy active at 100* / Non toxic	Cathepsin inhibitor B/L	*Pre-Clinical*	Sigma Aldrich
	Methyl-ß-cyclodextrin	*Not calculated, but active at 1000*	Cholesterol-removing agent, lipid raft disruption	*Not approved*	Sigma Aldrich
	NB-DNJ	*Not calculated, but active at 100* / Non toxic	Inhibits ceramide- glucosyltransferase and β-glucosidase 2	Gaucher disease & Juvenile Sandhoff disease	Calbiochem
	3' Sialyllactose Na Salt	Not Active / Non toxic	Inhibits viral binding	*Pre-Clinical*	Carbosynth
	Niclosamide	Not Active / > 9	Beclin-1 stabilizer in autophagy	Helmints	Selleckchem
	Ciclesonide	Not Active / > 20	Glucocorticoid	Asthma	Selleckchem
	Arbidol HCl	Not Active / > 40	Fusion inhibitor?	Influenza	Selleckchem
	Tofacitinib (Xeljanx)	Not Active / Non toxic	JAK inhibitor	Rheumatoid arthritis	Pfizer
	Baricitinib	Not Active / > 85	JAK inhibitor	Rheumatoid arthritis	Selleckchem
	Camostat	Not Active / Non toxic	TMPRSS2 inhibitor	Chronic pancreatitis	Merck
	Alfa-1 Antitrypsin	*Not calculated, but partially active at 12.5 mg/ml* / Non toxic	Cellular protease inhibitor	Alfa-1 antitrypsin deficiency	Grifols

Supplementary Table 1

DRUG 1	DRUG 2	DRUG 3	DRUG 4	Synergy	Toxicity in combination
Hydroxy-Cloroquine	Azithromycin			No	Similar
	Lopinavir			No	Similar
	Tipranavir			No	Similar
	Amprenavir			No	Similar
	Darunavir			No	Similar
	Baricitinib			No	Similar
	Tenofovir	Emtricitabine		No	Similar
	TAF	Emtricitabine		No	Similar
Remdesivir	Hydroxychloroquine			No	Similar
	Amantadine			No	Similar
	Chlorpromazine			No	Similar
	Baricitinib			No	Higher
	Tipranavir	Lopinavir		No	Similar
Lopinavir	Ritonavir			No	Higher
	Tipranavir			No	Higher
	Ritonavir	Tenofovir	Emtricitabine	No	Similar
	Ritonavir	Tenofovir Alafenamide	Emtricitabine	No	Similar
Tipranavir	Tenofovir	Emtricitabine		No	Similar
Tenofovir	Emtricitabine			No	Similar
Nelfinavir Mesylate Hydrate	Hydroxychloroquine			No	Similar
	Remdesivir			No	Similar
MDL28170	Hydroxychloroquine			No	Similar
	Remdesivir			No	Similar
	Nelfinavir Mesylate Hydrate			No	Similar
Plitidepsin	Hydroxychloroquine			No	Similar
	Remdesivir			No	Similar
	MDL 28170			No	Similar
	Nelfinavir Mesylate Hydrate			No	Similar

Supplementary Table 2

ACTIVITY	DRUG	IC_{50} / CC_{50} µM (Mean +/-SD)	Mode of Action	Previous Clinical Use	Vendor Origen
POST-ENTRY	Remdesivir	2.16 +/-4.1 / > 85	RNA Polymerase inhibitor	Ebola Virus	Cayman Chemical
	Galdesivir	Not Active / 100	RNA Polymerase inhibitor	YFV	MedChemExpress
	Favipiravir	*Not calculated, but partially active at 100* / Non toxic	RNA polimerase inhibitor	Flavivirus, Arenavirus, Bunyavirus, Alphavirus	Quimigen
	Saquinavir	Not Active / > 28	Protease inhibitor	HIV-1	Reference standard HPLC
	Lopinavir	*Not calculated, but active at 20* / > 87	Protease inhibitor	HIV-1	Abbot
	Ritonavir	*Not active* / 20-100	Protease inhibitor	HIV-1	Abbot
	Tipranavir	*Not calculated, but active at 20* / > 70	Protease inhibitor	HIV-1	Reference standard HPLC
	Nelfinavir Mesylate Hydrate	*Not calculated, but active <10* / > 25	Protease inhibitor	HIV-1	Sigma Aldrich
	Amprenavir	*Not calculated, but active at 100* / Non toxic	Protease inhibitor	HIV-1	GSK
	Fosamprenavir Calcium	Not Active / > 25	Protease inhibitor	HIV-1	Sigma Aldrich
	Darunavir	*Not calculated, but partially active at 100* / Non toxic	Protease inhibitor	HIV-1	Sigma Aldrich
	Atazanavir Sulfate	Not Active / > 20	Protease inhibitor	HIV-1	Reference standard HPLC
	Tenofovir disoproxil fumarate	Not Active / > 100	Reverse Transcriptase inhibitor	HIV-1	Selleckchem
	Emtricitabine (Emtriva)	Not Active / Non toxic	Reverse Transcriptase inhibitor	HIV-1	Gilead
	Tenofovir Alafenamide	Not Active / Non toxic	Reverse Transcriptase inhibitor	HIV-1	Selleckchem
	Velpatasvir	Not Active / > 10	Protease inhibitor	HCV	Selleckchem
	Sofosbuvir	Not Active / Non toxic	Protease inhibitor	HCV	Selleckchem
	Boceprevir	Not Active / Non toxic	Protease inhibitor	HCV	Quimigen
	Vesatolimod	Not Active / > 20	TLR7 agonist	Hepatitis & HIV-1	MedChemExpress
	Interferon 2 alfa	8.1+/-0.7 $x10^2$ IU/mL / Non toxic	IFN stimulated antiviral proteins	Hepatitis & HIV-1	Sigma-Aldrich
	Interferon gamma	11.2 $x10^2$ IU/mL / Non toxic	IFN stimulated antiviral proteins	Granulomatous disease	Sigma-Aldrich
	Plitidepsin	0.06 +/- 0.02 / > 0.1	Targets eukaryotic Elongation Factor 1A2 (eEF1A2)	Multiple myeloma	PharmaMar

Supplementary Table 3

Bioinformatic ANALYSIS	DRUG	IC_{50} / CC_{50} µM (Mean +/-SD)	Mode of Action	Previous Clinical Use	Vendor Origen
	Salbutamol	Not Active	Predicted SARS-Cov-2 Protease inhibitor	Asthma	Sigma Aldrich
	Diclondazolic acid (Lonidamine)	Not Active	Predicted SARS-Cov-2 Protease inhibitor	Anticancer	Abcam
	Thiocolchicoside	Not Active	Predicted SARS-Cov-2 Protease inhibitor	Skeletal muscle relaxant	Sigma Aldrich
	Morphothiadine	Not Active / 54	Predicted SARS-Cov-2 Protease inhibitor	Hepatitis B	Quimigen
	Ingliforib	Not Active	Predicted SARS-Cov-2 Protease inhibitor	Glycogen phosphorylase inhibitor	Quimigen
	Perampanel	Not Active	Predicted SARS-Cov-2 Protease inhibitor	Antiepileptic	Quimigen
	Montirelin trifluoroacetate salt	Not Active	Predicted SARS-Cov-2 Protease inhibitor	Thyrotropin-releasing hormone agonists	Sigma Aldrich
	Saquinavir	Not Active	Predicted SARS-Cov-2 Protease inhibitor	HIV-1	Reference standard HPLC
	Pamicogrel	Not Active / 6.4	Predicted SARS-Cov-2 Protease inhibitor	Antiplatelet aggregation	Quimigen
	Pomalidomide	Not Active	Predicted SARS-Cov-2 Protease inhibitor	Anticonvulsants	Sigma Aldrich
	Laflunimus Sodium Salt	Not Active	Predicted SARS-Cov-2 Protease inhibitor	Anti-inflammatory	Quimigen

Supplementary Table 4

ACTIVITY	DRUG	IC_{50} / CC_{50} µM (Mean +/-SD)	Mode of Action	Previous Clinical Use	Vendor Origen
UNKNOWN	Azithromycin (Zitromax)	Not Active / Non toxic	Antibiotic	Bacteria	Pfizer
	Doxycycline (Anaclosil)	Not Active / Non toxic	Antibiotic	Bacteria	Reig
	Eravacycline (Xerava)	Not Active / Non toxic	Antibiotic	Resistent bacteria	Tetraphase Pharmaceuticals
	Quinacrine dihydrochloride	Not Active / > 6	Inhibitor of NF-kappaB	Parasites	Sigma Aldrich
	Ivermectin (Stromectol)	Not Active / > 2	Nuclear import inhibitor	Parasites	MSD
	Mefloquine hydrochloride	Not Active / Non toxic	Phospholipid bilayer?	Malaria	Sigma Aldrich
	N-Acetil cystein (Flumil)	Not Active / Non toxic	Synthesis of glutathione	Influenza	Zambon
	Itraconazole	79.37 / Non toxic	Inhibits OSBP, which produces the membrane-bound viral replication organelles	Fungus	Janssen
	Fluconazol	Not Active / Non toxic	Antibiotic	Fungus	Franesius Kabi
	Famotidine	Not Active/ Non toxic	Histamine-2 receptor antagonist	Gastric	Normon
	Cetirizine dihydorcloride	Not Active/ Non toxic	Histamine-H1 receptor antagonist	Antihistaminic	Sigma Aldrich
	Colchicine	Not Active / 0.63	Anti mytotic	Gout attacks	Merck
	Palbociclib	Not Active/ 2,7	CDK4/6 inhibitor	Breast cancer	Selleckchem
	Ribociclib	Not Active / > 20	CDK4/6 inhibitor	Breast cancer	Selleckchem
	Abenaciclib	Not Active / > 1	CDK4/6 inhibitor	Breast cancer	Selleckchem
	Silibinin	Not active / Non Toxic	?	Liver disease	Rottapharm Madaus
	Atorvastatin	Not active / Non Toxic	HMG-CoA reductase inhibitor	Cardiovascular disease	Normon
	Fenofibrate	19.8+/- 8 / Non Toxic	Activates PPARα	Dyslipidemia	Lacer
	MDL 28170	0.14 +/- 0.06 / > 87	Calpain III inhibitor & Cathepsin B inhibitor	*Pre-Clinical*	Merck
	NPO-2142; -2143 & -2260	~ 0.54 / Non toxic	Calpain & Cathepsin inhibitors	*Pre-Clinical*	Landsteiner Genmed
	NPO-2138	*Not calculated, but partially active at 100* / Non toxic	Calpain & Cathepsin inhibitors	*Pre-Clinical*	Landsteiner Genmed

Supplementary Table 5